Retrofitting of Several Cell Technologies Using a Protruding Collector Bar Cathode Assembly

Wei Liu[1], Zhibin Zhao[2], Ming Liu[3], Xi Cao[2], Hongwu Hu[3], Yafeng Liu[4] and Marc Dupuis[5]

1. Senior engineer, Manager of R&D Department
2. Senior engineer
3. Senior engineer, Deputy director of Reduction Department
4. Chief engineer of CHINALCO

Shenyang Aluminum & Magnesium Engineering & Research Institute Co. Limited (SAMI), Shenyang, China

5. Consultant, GéniSim Inc., 3111 Alger St., Jonquière, Québec, Canada G7S 2M9

Corresponding author: drmarcdupuis@gmail.com

Abstract

Since 2015, SAMI has been involved in several cell retrofits: SY200, SY235, SY300, SY400, SY500, GP500, NEUI500 and SY600. In all those retrofits, SAMI's cathode lining redeveloped with SAMI's New Conceptual Cathode Technology ("NCCT") has been used. For the first time the NCCT will be described here, it involves using a protruding collector bar cathode assembly, cast iron rodding and comes with a gas preheating procedure for the steel bar and carbon block. SAMI's NCCT was successfully adapted to different grades and sizes of cathode blocks over more than 2600 cells so far. Modeling results of the conception work will be presented but more importantly, KPI improvement of the retrofitted cells will also be presented.

Keywords: Aluminium, Modeling and simulation, Cell retrofit, KPI, Cast iron rodding, Gas preheat

1. Introduction

Reference [1] is presenting SAMI's retrofit of the GAMI's GP350 into the SY370 at QTX smelter in China. That retrofit involved the addition of two compensation loops to reduce the Bz intensity and the introduction of SAMI's proprietary Horizontal Current Reduction Technology ("HCRT") cathode technology to reduce the horizontal current in the metal pad.

References [2] and [3] are presenting SAMI's retrofit of the SM-17SE into the SY240 at Inalum smelter in Indonesia. That retrofit involved the introduction of SAMI's proprietary NCCT cathode technology to reduce the horizontal current in the metal pad. The NCCT cathode technology is not described in [2] and [3] but it will be fully described in here.

SAMI started to work on the NCCT cathode technology in 2010 so just after the development of the HCRT cathode technology. HCRT is based on split bar technology [4] and [5] while NCCT is based on the usage of protruding collector bar cathode assembly, the design concept will be presented below. What also differentiate NCCT from HCRT is the introduction of cast iron rodding in NCCT. As presented in [1], HCRT cathode technology reduces the horizontal current by about 30 % while NCCT cathode technology reduces the horizontal current by about 40 % as presented in [2] and [3].

SAMI used NCCT cathode technology to retrofit several smelters in China using a wide variety of cell technologies. The resulting gains will be presented here altogether with the new resulting KPI. But before, that the modeling work and the design concept will be presented.

2. Thermo-Electric Modeling Work to Reduce Horizontal Current

The aim or the NCCT development work was to reduce the metal pad horizontal current by more than the 30 % already achieve by HCRT. To achieve that goal, it was decided to try to replace the traditional mix rodding by cast iron rodding. This change was first investigated in the 3D thermo-electric full cell slice model. Figure 1 is presenting the model mesh. Figure 2 is presenting the resulting temperature and converged ledge profile, while Figure 3 is presenting the resulting metal pad current density for the case of the SY240 as already presented in [2].

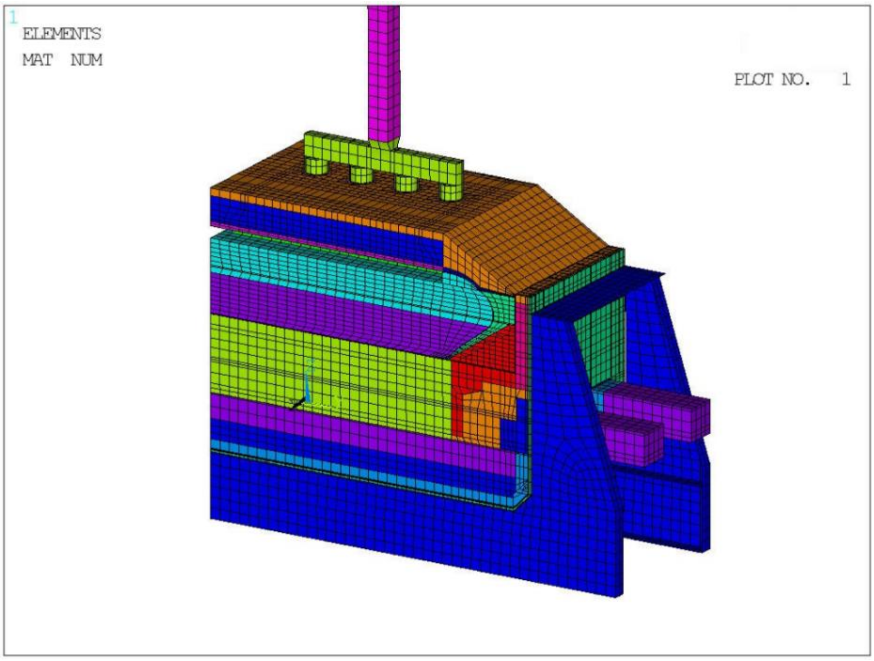

Figure 1. Thermo-electric 3D full cell slice model mesh.

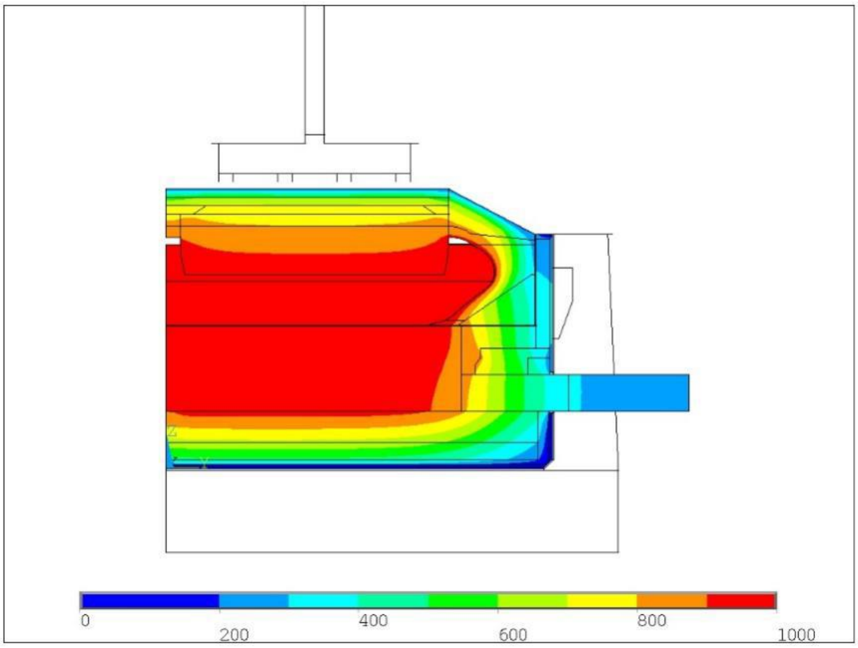

Figure 2. Thermo-electric 3D full cell slice model isotherms (°C).

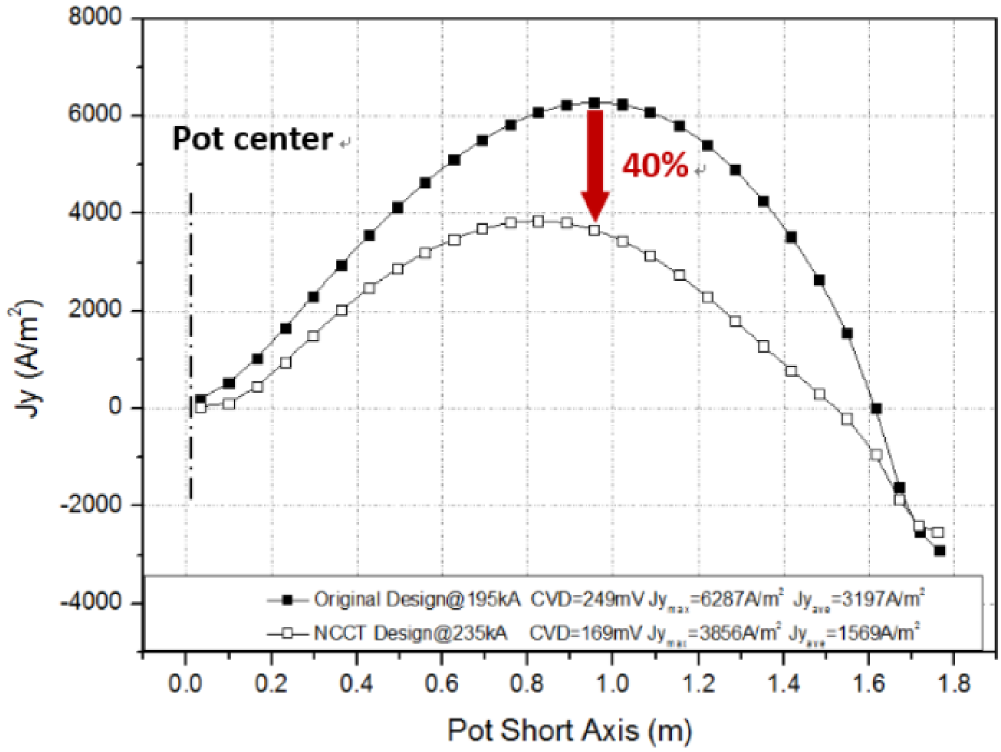

Figure 3. Thermo-electric 3D full cell slice model metal pad horizontal current.

3. MHD Cell Stability Analysis Modeling Work at Reduced Horizontal Current

The impact of the reduced horizontal current is studied next using the MHD cell stability shallow water model. The metal pad horizontal current is recalculated first in the MHD model. Figure 4 is presenting the obtained horizontal current for the SY500 cell before the introduction of NCCT. Figure 5 is presenting the resulting steady-state metal flow while Figure 6 is presenting the resulting steady-state bath metal interface.

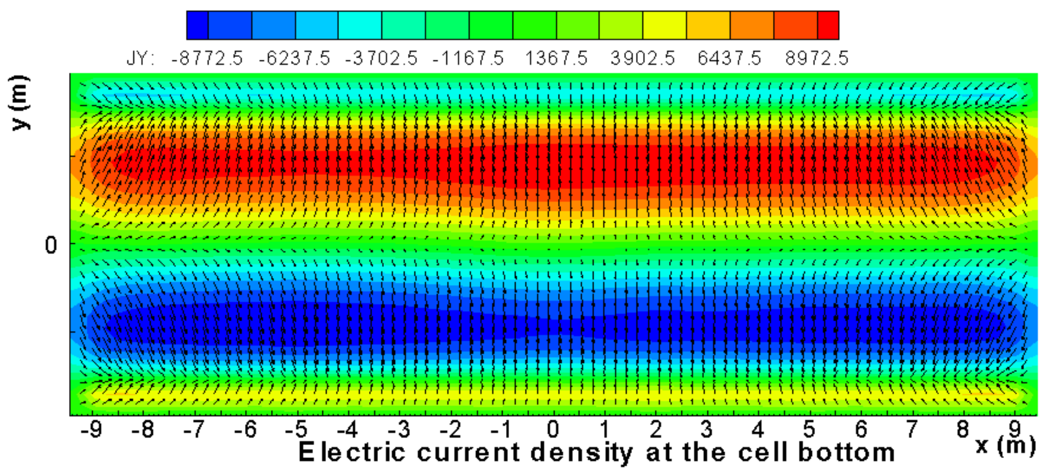

Figure 4. MHD-Valdis model metal pad horizontal current before NCCT.

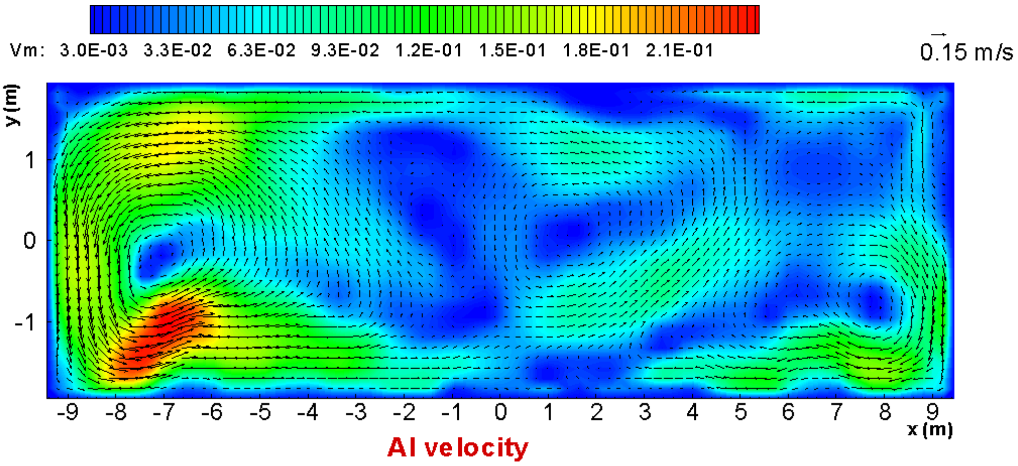

Figure 5. MHD-Valdis model metal pad steady-state flow before NCCT.

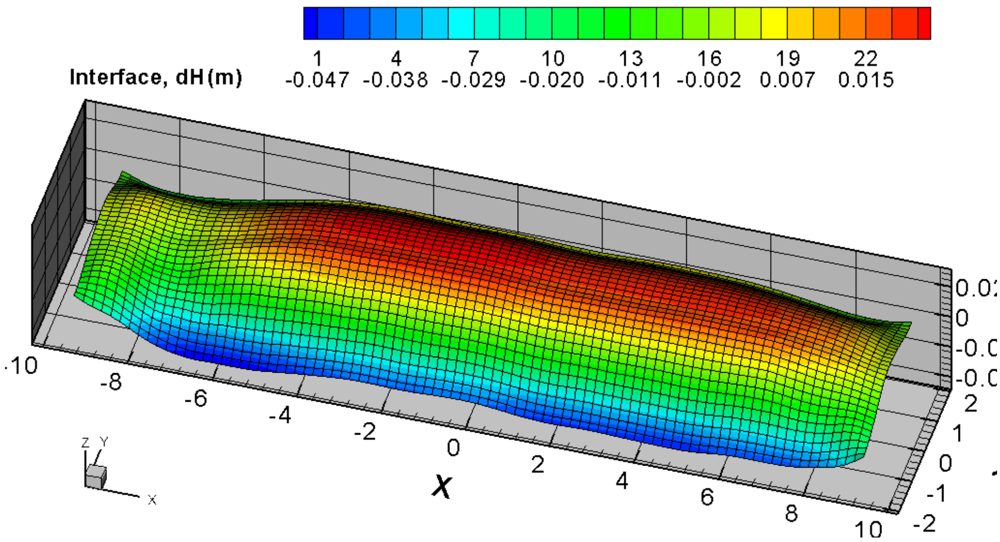

Figure 6. MHD-Valdis model steady-state bath-metal interface before NCCT.

Those steady-state results are not providing any direct indication of cell stability. In order to obtain that, a transient cell stability analysis must be carried on. Figure 7 presents the resulting cell stability prediction for 4 values of anode-cathode distance (ACD). According to the analysis, the SY500 cell before NCCT is stable up to 36 mm of ACD but become unstable at 35 mm ACD.

As Figure 8 indicates, the introduction of NCCT very significantly reduces the intensity of the horizontal current in the metal pad. As indicated in Figure 9 and Figure 10, the steady state metal velocity and the bath/metal interface deformation are both being reduced by that reduction of the horizontal current intensity. But looking only at the changes in the steady state results, it is not possible to tell much about the possible gain of cell stability.

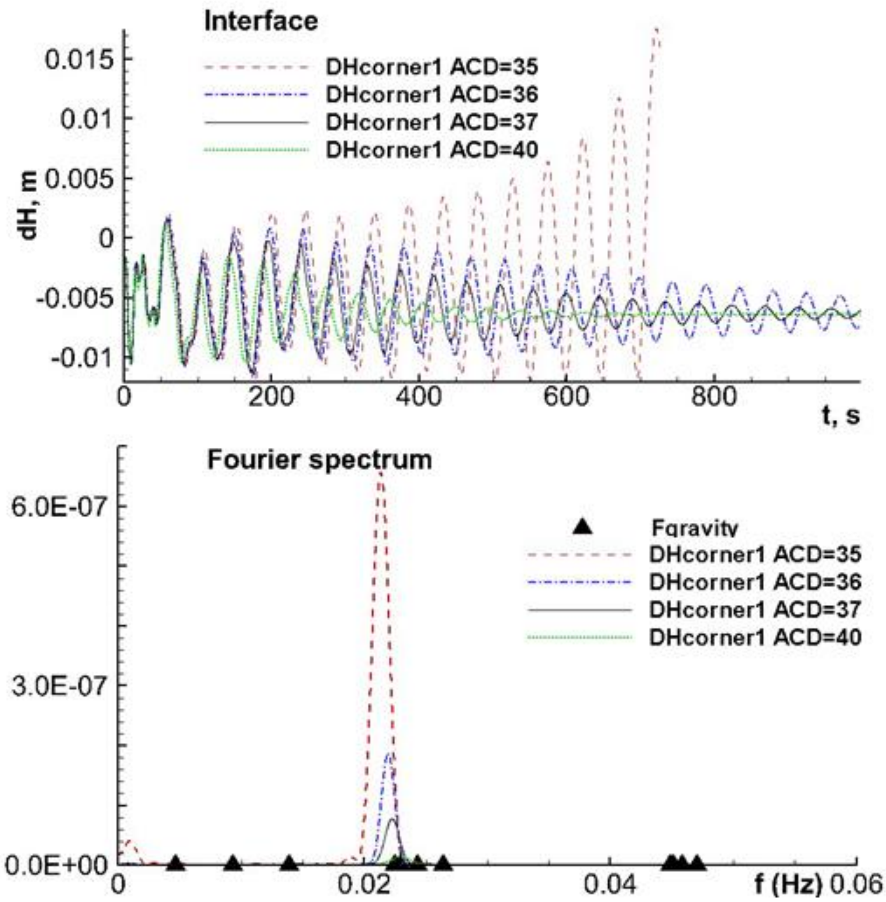

Figure 7. MHD-Valdis model transient cell stability analysis before NCCT.

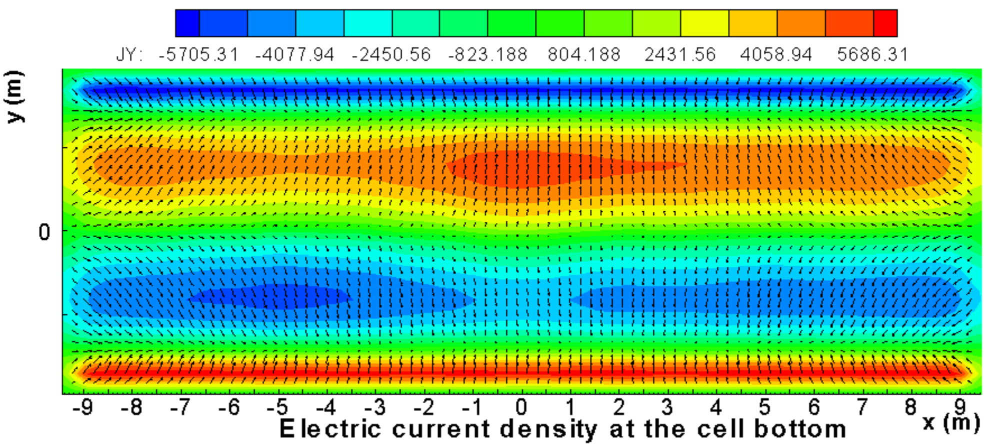

Figure 8. MHD-Valdis model metal pad horizontal current after NCCT.

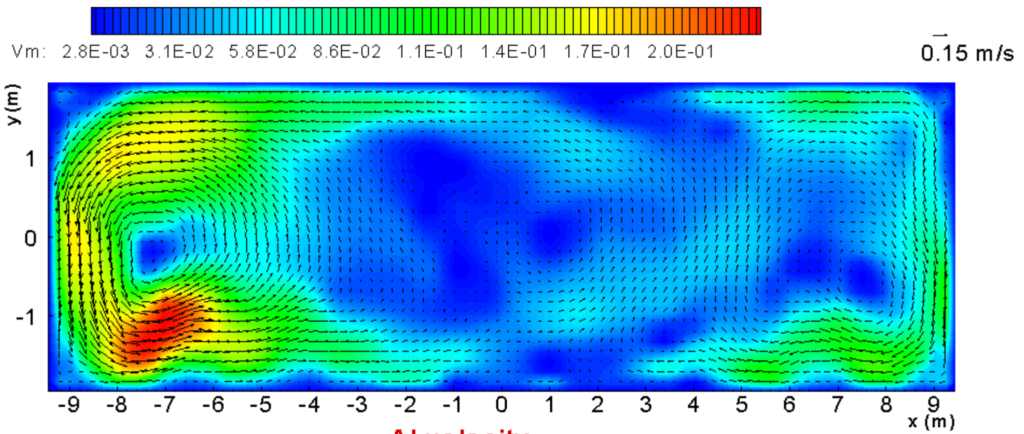

Figure 9. MHD-Valdis model metal pad steady-state flow after NCCT.

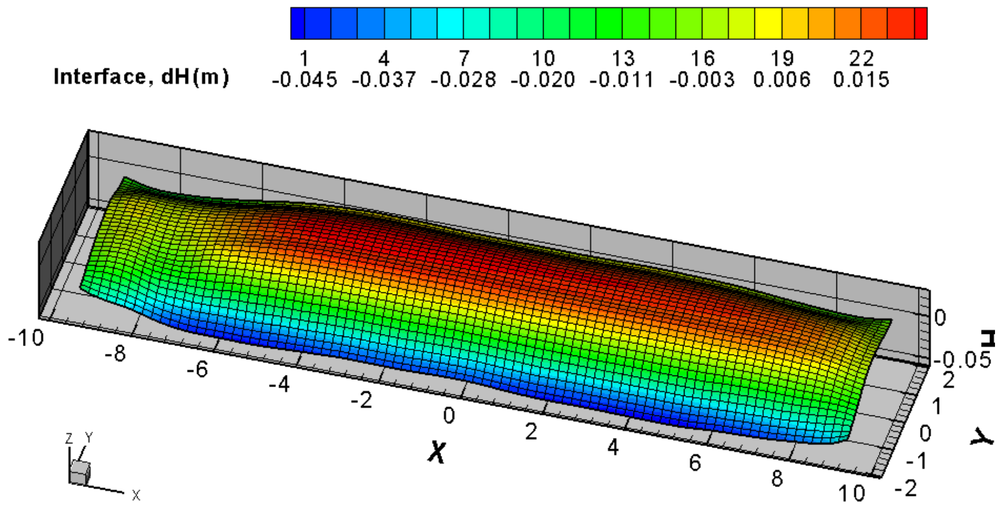

Figure 10. MHD-Valdis model steady-state bath-metal interface after NCCT.

Figure 11 presents a second cell stability analysis performed after an update of the code. As explained in [6], MHD-Valdis had to be modified to be able to analyze the cell stability at very low ACD values. A new parameter related to the anode burnoff adjustment procedure was added. While the stability analysis presented in Figure 7 was done using a constant metal pad thickness of 18 cm and an initial perturbation amplitude of 5 mm, the stability analysis presented in Figure 11 was performed as at constant 26 mm ACD, an initial perturbation amplitude of 1 mm using the new code version with the new anode burnoff adjustment option activated. The retrofitted SY500 cell with NCCT is predicted to be stable at 26 mm ACD with 19 cm or more of metal pad thickness.

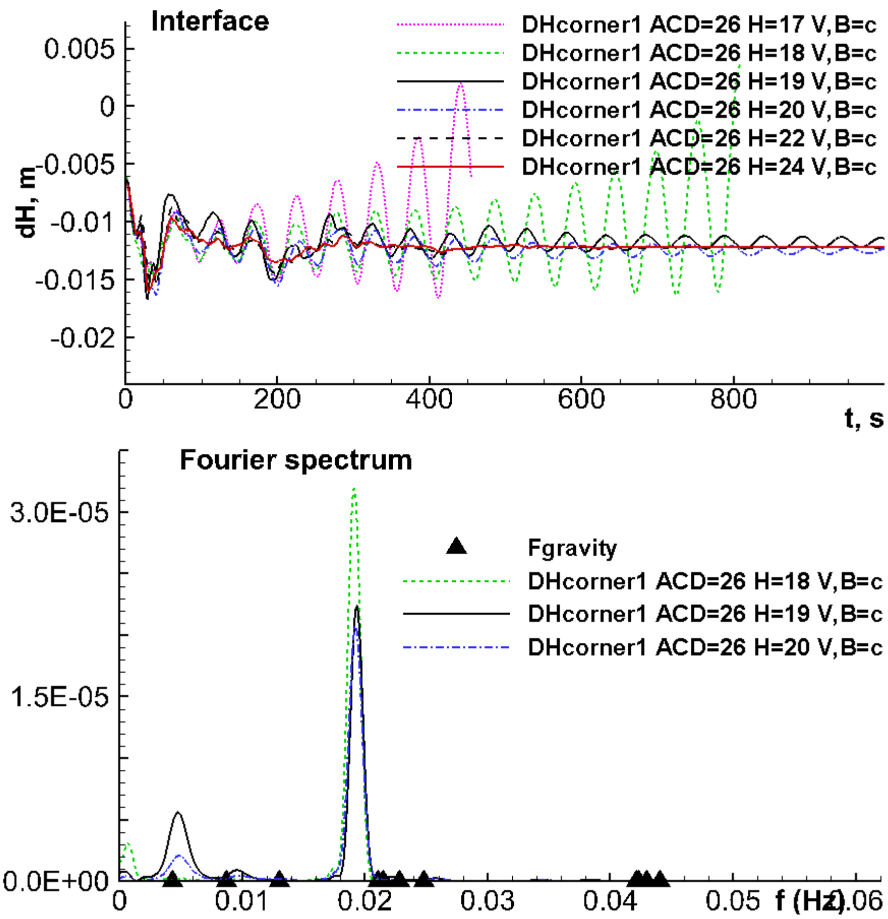

Figure 11. MHD-Valdis model transient cell stability analysis after NCCT.

4. Transient Thermo-Mechanical Cast Iron Rodding Model

A transient thermo-mechanical model similar to the one presented in [6] was developed to study the thermal stresses developing during the cast iron rodding procedure in order to develop a gas preheating procedure and a slot design that prevent the cracking of the cathode block during the rodding. Figure 12 presents the maximum stress prediction after the cast iron rodding of a graphitic cathode block of the SY500 after gas preheating at 400 ºC on the left and 500 ºC on the right.

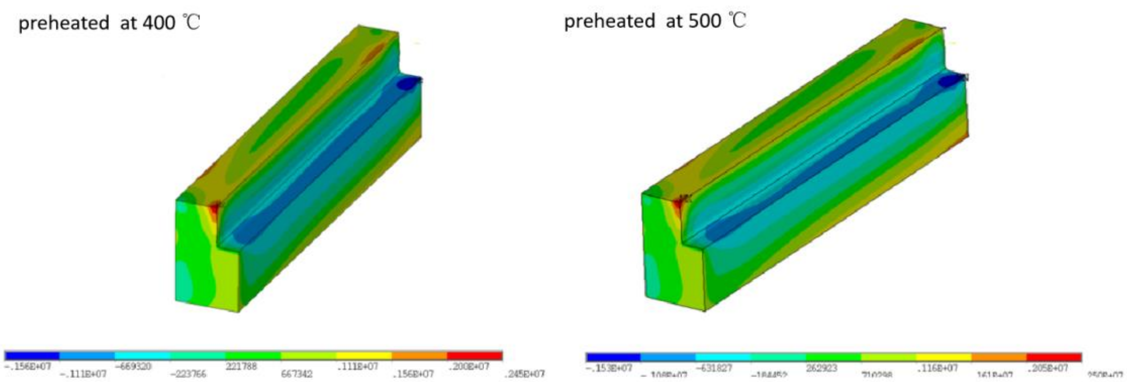

Figure 12. Stress distribution of the graphitic blocks preheated at 400 °C and 500 °C.

As it is indicated in [7], the radius of the cathode slot corners is very important to reduce the local stresses in those corners and to reduce the risk of crack formation. Figure 13 presents the evolution of local stress for two slot corner radii.

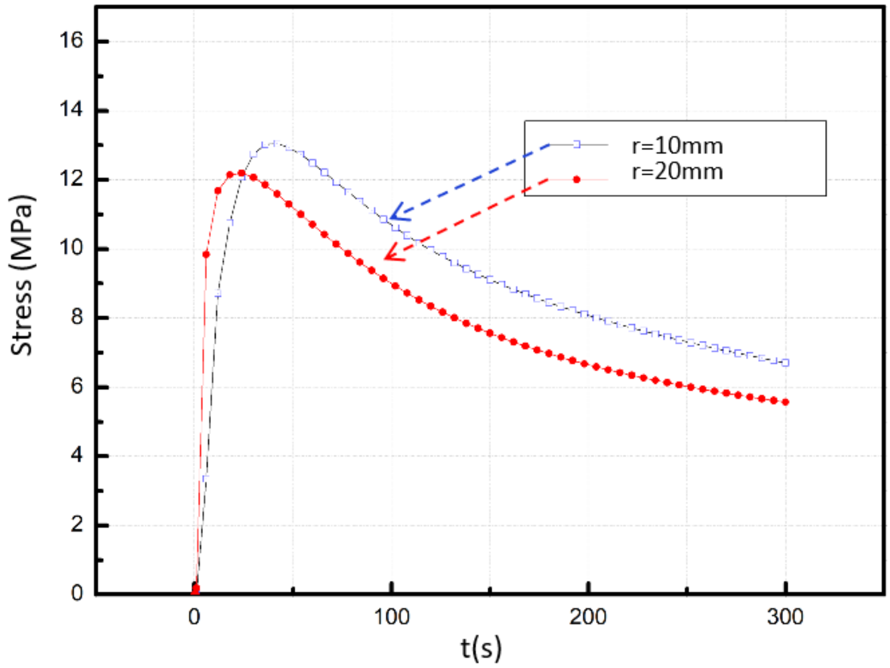

Figure 13. Local stress evolution during rodding for two slot corner radii.

5. Protruding Bar Cathode Assembly Design

In order to reduce the horizontal current in the metal pad, a new cathode assembly design was developed with the help of the above modeling tools. In order to achieve that goal, the resistance of the collector bar must be reduced. In order to reduce that collector bar resistance, it was decided to increase the collector bar section significantly. Finally, in order to avoid reducing the height of carbon above the bar to let the bar protrude out of the cathode block as displayed in Figure 14. As described in [8], the addition of the barrier material around the protruding part of the collector bar is also part of the NCCT assembly design. Replacing mix rodding by cast iron rodding that is part of the new design also contributed to reduce the global resistance of the cathode assembly leading to a reduce CVD of the cell in operation.

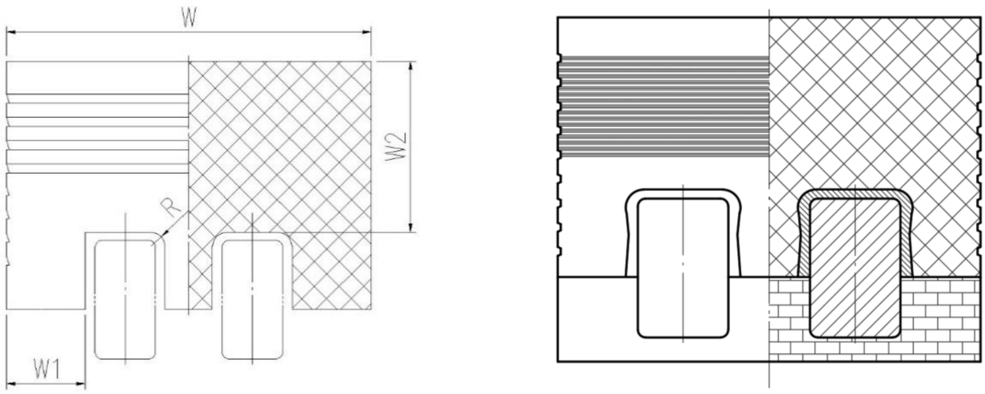

Figure 14. Schematics of the protruding collector bar cathode assembly.

The important parameters of the design are presented in Figure 14: W is the width of the block, W1 is the flange width, W2 is the effective height of the block and R is the radius of the slot corner.

W1 and W2 determine the strength of the cathode carbon block; W2/W1 directly determines the cracking direction during rodding and W2 is an important parameter related to longer pot life. In order to assure the block's service life, the experiences show that W1 shall not be less than 120mm, W2 shall not be less than 280mm, and the ratio of W2/W1 shall not be less than 2.0.

R is an important factor that directly determines the probability of wing crack. As already shown in Figure 13, the calculated results show that the first principal stress of the slot when the radius of 20 mm is significantly less than that when the radius of 10mm.

6. Cast Iron Rodding Procedure

A cast iron rodding procedure that prevents cathode block cracking and ensure a long lining life was developed as part of the NCCT package. The first step involved the development of a gas preheating system and gas preheating procedure. The second step involved the development of a cast iron rodding procedure.

6.1 Gas Preheating System and Gas Preheating Procedure

A gas-fired preheating system divided into multiple temperature zones in horizontal and vertical directions has been developed. Temperature measuring devices are set on each temperature zone to monitor the temperature in real time. The control system adjusts the proportion and addition of fuel and combustion supporting agent through the feedback signal of the temperature measuring device, so as to control the heating rate and temperature distribution of the bar/block. This is visualized through the HMI (Human Machine Interface) shown in Figure 15 (left).

Figure 15 (right) is showing two cathode assemblies ready to be preheated by the preheating system located just behind ready to be placed on top of the blocks to start the preheating procedure. Based on the modeling results presented in Figure 12, it was decided to preheat the bar up to 700 °C and the block up to 600 °C at the top and 500 °C at the bottom. Around 7 or 8 of such preheating cycles can be performed each day by that preheating system. The fuel consumption is less than 50 m³ of natural gas per block.

Figure 15. Gas preheating system. Left: HMI display. Right: preheating system

6.2 Cast Iron Rodding Procedure

Figure 16 presents two tested cast iron casting sequences. According to the statistical results of 500 cases of cast iron casting (cast in mode 1 and mode 2 respectively), the casting success rate (without casting cracks) of mode 2 is 1 % higher than that of mode 1. The difference between mode 1 and mode 2 is that in mode 2, the casting time interval between two adjacent casting position in the width direction of carbon blocks is shorter. Before that the thermal shock caused by pouring the hot cast iron reaches its maximum stress level in the cathode block, the adjacent casting position is performed producing heating coming from the opposite direction which reduces the stress generated by the initial pour. That step-by-step casting procedure reduces the intensity of the thermal stresses by increasing the thermal uniformity of the cathode block.

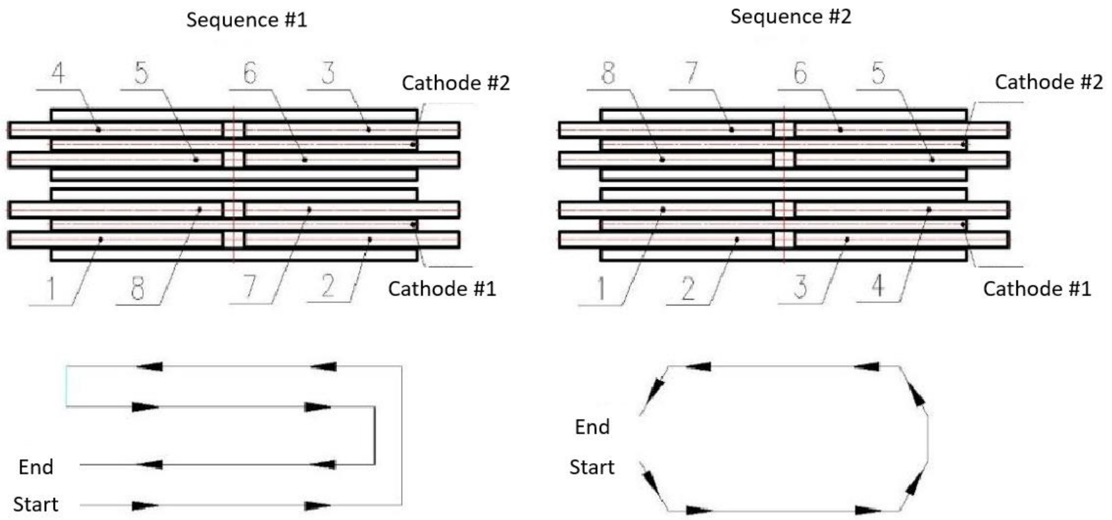

Figure 16. Cast iron casting sequences. Left: mode 1. Right: mode 2.

Figure 17 (left) presents the NCCT cathode assembly after cast iron rodding. The final step before those cathode assembly would be ready to be put in a cell is to cast the refractory material shown in Figure 14 (right). Figure 17 (right) presents the NCCT cathode assembly after that final step.

Figure 17. NCCT cathode assembly. Right: after cast iron rodding. Left: ready to be put in a cell.

7. Obtained KPIs for Many Cells Retrofitted Using NCCT

NCCT is widely applicable to a new smelter construction and existing smelter upgrading of 200 to 660 kA electrolytic cells for smelters located both inside and outside China. At present, the technology has been applied in 8 smelters in China and 2 smelters outside China (Turkey and Indonesia). The number of electrolytic cells has exceeded 2 600, and more than 40 000 graphitized and graphitic cathode carbon blocks of different cell types have been cast and assembled.

Table 1 shows that the electrolytic cells adopting this technology, especially the high-capacity electrolytic cell, have reached 2 400 days since it was started in October 2015, and the electrolytic cells are still running stably and healthily. According to the performance of the electrolytic cells, combined with the operation and operational data of the previous electrolytic cells, the expected life of the electrolytic cells will exceed 2 600 days.

Table 1. Some cases of industrial application of NCCT.

Cell kA	Smelter name	Tech-nology	Num. of cells	Cathode block grade*	CVD mV	mV gain to reference	Startup date
500	Xinjiang Agricultural Sixth Division	SY500	7	50 % graphitic/ Graphitized	260/ 190	60-130	2015/10
200	Chalco Qinghai Branch	SY200	52	50 % graphitic	220	60	2016/1
235	Inalum	SY240	3	Graphitized	169	80	2017/3
300	Turkey ETI Aluminium	SY300	23	50 % graphitic	230	50	2019/1
400	Xinjiang Tianlong	SY400	96	50 % graphitic	240-280	55-85	2016/8
500	Inner Mongolia Huayun Phase I	SY500	342	50 % graphitic	265	50-70	2017/5
500	Yingkou Zhongwang	SY500	320	Graphitized	185	50-60	2018/9
500	Guangxi Hualei	GP500	62	50 % graphitic	240	50-60	2020/10
640	Shandong Xinfa	SY600	636	50 % graphitic	240	60-70	2016/1

*Graphitic cathode blocks have typically 30 %, 50 % or 100 % of graphite; this has to be specified to know the block grade.

The reduction of CVD is around 50–70 mV when the cathode grade is kept the same and can reach 130 mV when the cathode grade is also changed from semi-graphic to graphitized. Table 2 shows the new KPIs after adoption of NCCT. The average KPI values of the full set are 93.7 % current efficiency and 12.6 kWh/kg Al. For the 3 SY500 smelters in particular, the average KPI values are 94.3 % current efficiency and 12.5 kWh/kg Al, while the reported KPIs for the SY500 without NCCT [9] are 92.0 % current efficiency and 12.8 kWh/kg Al so a reduction of 0.3 kWh/kg Al indicating the clear benefit of adopting NCCT.

Table 2. New KPI after adoption of NCCT.

Cell kA	Smelter name	Technology	Production t Al/cell-day	Current Efficiency %	Cell Voltage V	DC Energy Consumption kWh/t Al
500	Xinjiang Agricultural Sixth Division	SY500	3.756	93.3	3.860	12332
200	Chalco Qinghai Branch	SY200	1.567	90.54	3.769	12408
235	Inalum	SY240	1.819	96.11	4.094	12697
300	Turkey ETI Aluminium	SY300	2.328	95.12	4.071	12757
400	Xinjiang Tianlong	SY400	3.016	91.6	3.952	12862
500	Inner Mongolia Huayun Phase I	SY500	3.792	94.18	3.92	12406
500	Yingkou Zhongwang	SY500	3.801	94.4	4.006	12650
500	Guangxi Hualei	GP500	3.794	94.23	3.945	12480

8. Conclusions

The NCCT involves using a protruding collector bar cathode assembly, cast iron rodding and comes with a gas preheating of the steel bar and carbon block technology. It can reduce the CVD and horizontal current of cells at the same time.

Now, SAMI's NCCT has been successfully adapted to different grade and size of cathode blocks in over more than 2 600 cells, including new construction and technical upgrading of 200–660 kA electrolytic cells with good performances as demonstrated by the KPI improvements.

9. References

1. Marc Dupuis and Kangjian Sun, Review of the SAMI retrofit project in QTX smelter in China. *Proceedings of the 39th International ICSOBA Conference*, Virtual Conference, 22-24 November 2021, *Travaux* 50, 671-678.
2. Ming Liu et al., The successful modernization of SM-17SE pot in Inalum, *12th Australasian Aluminium Smelting Technology Conference Queenstown, New Zealand*, 2018, 1-9.
3. Ming Liu et al., Amperage increase from 195 to 240 kA through pot upgrading, *Light Metals*, 2019, 583-591.
4. Shengyang Al and Mg Eng. Res. Inst., China patent, CN102453927A (2012).
5. Wenjo Tao et al., Impact of the usage of a slotted collector bar on thermoelectric field in a 300-kA aluminum reduction cell, *JOM*, Vol. 67, No. 2, 2015, 322-329.
6. Valdis Bojarevics and Marc Dupuis, Application and adaptability of MHD stability computation for modern aluminium reduction cells at extreme conditions of low ACD, *Light Metals*, 2021, 565-571.
7. Bénédicte Allard et al., Modelling of collector bar sealing in cathode blocks with cast-iron, *Light Metals*, 2009, 1097-1102.
8. Shengyang Al and Mg Eng. Res. Inst., China patent, CN203333778U (2013).
9. Alton Tabereaux and Marc Dupuis, Key Performance indicator comparisons of global state-of-the-art aluminium cell technologies, *Aluminium World Journal*, 2019, 14-20.